Polymer Chemistry

Accepted Manuscript

ROYAL SOCIETY OF CHEMISTRY

www.rsc.org/polymers

Journal Name

RSCPublishing

ARTICLE

Porphyrin-containing Amphiphilic Block Copolymer for Photodynamic Therapy

Cite this: DOI: 10.1039/x0xx00000x

Lei Xu, Lichao Liu, Feng Liu*, Haibo Cai, Weian Zhang*

Received ooth January 2012,
Accepted ooth January 2012

DOI: 10.1039/x0xx00000x

www.rsc.org/

Amphiphilic PNIPAM-*b*-PTPPC6MA block copolymers were first synthesized using porphyrin-containing monomers. The mono-hydroxylphenyl-triphenylporphyrin photosensitizer, TPP-OH, was modified into porphyrin monomer, and it was further used to construct the amphiphilic PNIPAM-*b*-PTPPC6MA block copolymers using RAFT polymerization. PNIPAM-*b*-PTPPC6MA block copolymers can self-assemble into a plethora of morphologies ranging from spheres to vesicular aggregates and further to single large vesicle. The PNIPAM-*b*-PTPPC6MA micelles exhibited a high singlet oxygen quantum yield. Moreover, confocal laser scanning microscopy (CLSM) and flow cytometry analysis confirmed PNIPAM-*b*-PTPPC6MA micelles could effectively enhance the internalization rate in MCF-7 cells. According to the MTT assay, PNIPAM-*b*-PTPPC6MA micelles exhibited low dark toxicity and efficient PDT efficacy to MCF-7 cells. Thus PNIPAM-*b*-PTPPC6MA block copolymers have the potential application for photodynamic therapy.

Introduction

Recently, photodynamic therapy (PDT) has become one of outstanding protocols for cancer treatment which involves accumulation of photosensitizer (PS) into cancer cells, irradiation with the light of appropriate wavelength and the coexistence of molecular oxygen.[1-5] During PDT, the activated PS could react with the oxygen in the tissue under irradiation, causing the formation of cytotoxic species such as singlet oxygen, resulting in toxicity to malignant cells.[6] Thus PS plays an important role in PDT treatment which determines the efficiency of PDT. Compared to chemotherapy, radiation, surgery and other therapeutic modalities, PDT is more controllable, less invasive and fewer side effects. Moreover, several commercial PSs including Photofrin® and Visudyne® approved by the U.S. Food and Drug Administration (FDA) have been utilized in clinical cancer treatments.[1,7-9]

Porphyrin and its derivatives have received great attention as the second generation of PS since they can effectively produce singlet oxygen and has a low side effect to the body.[10,11] However, porphyrin PSs still have not widely been applied in clinical PDT, since most of them are aromatic molecules, exhibiting non-selectivity, poor water solubility and limited bio-distribution.[12-15] To overcome these obstacles, much effort has been devoted to enhancing the properties of porphyrin PS. For example, Zheng *et al*. constructed the porphysomes by self-assembly of phospholipid-porphyrin conjugates, which have a liposome-like structure with advantageous properties such as high loading capacity and excellent biocompatibility, and these porphysomes exhibited potential applications in the photodiagnosis and phototherapy.[16-19] More recently, a variety of polymeric PSs have also been developed by several research groups, especially for the conjugation of PSs with hydrophiphilic polymers which can greatly increase the solubility of PSs in aqueous solution. Na *et al.* prepared a series of polymeric PSs using hydrophilic polymers such as hyaluronic acid, chondroitin sulfate, pluronic F127, polyethylenimine, and they found these polymeric PSs could effectively improve the solubility of the PSs and enhance cellular internalization.[20-23] Additionally, porphyrin molecules were also used as an initiator to prepare porphyrin-containing polymers.[24,25] For example, Lai *et al*. prepared star-shaped 4-armed porphyrin polylactide (PLLA) via ring-opening polymerization (ROP) of L-lactide using *meso*-tetra-(*p*-hydroxy methylphenyl) porphyrin as an initiator, and this porphyrin-PLLA PS could efficiently generate singlet oxygen under irradiation with much lower self-quenching, and would be promise for cancer therapy[26]. Additionally, porphyrin was also used as an initiator to produce porphyrin-containing star-shaped amphiphilic block polymers. A series of star-shaped amphiphilic poly(L-leucine)-*block*-polylysine diblock copolypeptides PSs bearing porphyrin for promising PDT have

been prepared by ROP of L-leucine and lysine using 5-(4-aminophenyl)-10, 15, 20-triphenyl-porphyrin as an initiator.[27] Although polymeric porphyrin PSs have been developed using different approaches, and they also exhibited promising application for PDT, we found there is few report on the construction of polymeric porphyrin PS using the porphyrin derivative as a monomer, especially for the porphyrin-containing block copolymers.

It is well-known that amphiphilic block copolymers have widely been applied in drug release system, since these delivery systems had high drug loading efficiency and more controllable drug release speed.[28-32] There are two main methods to construct the drug release system based on amphiphilic block copolymers. Small drug molecules could be encapsulated in assembled micelles of amphiphilic block copolymers, or they also could react with the reactive groups of preprepared block copolymers to form release system.[33] Here, we constructed porphyrin-containing amphiphilic poly(*N*-isopropylacrylamide) (PNIPAM) block copolymers using porphyrin derivative as a monomer, which would have a high drug loading efficiency. Additionally, PNIPAM as a typical temperature-responsive polymer has also been used for control drug release.[34,35]

In this contribution, a novel porphyrin monomer, TPPC6MA, was first synthesized, and then TPPC6MA was further used to construct the amphiphilic block copolymers, poly(N-isopropylacrylamide)-*block*-poly(TPPC6MA) (PNIPAM-*b*-PTPPC6MA) via reversible addition-fragmentation chain transfer (RAFT) polymerization. The self-assembly behavior of amphiphilic PNIPAM-*b*-PTPPC6MA block copolymers were studied by dynamic light scattering (DLS) and transmission electron microscopy (TEM). Cellular dark cytotoxicity and phototoxicity by the PNIPAM-*b*-PTPPC6MA micelles were evaluated in MCF-7 cells using MTT assay, and their biodistribution was comparable to free porphyrin using confocal microscopy and flow cytometry, respectively.

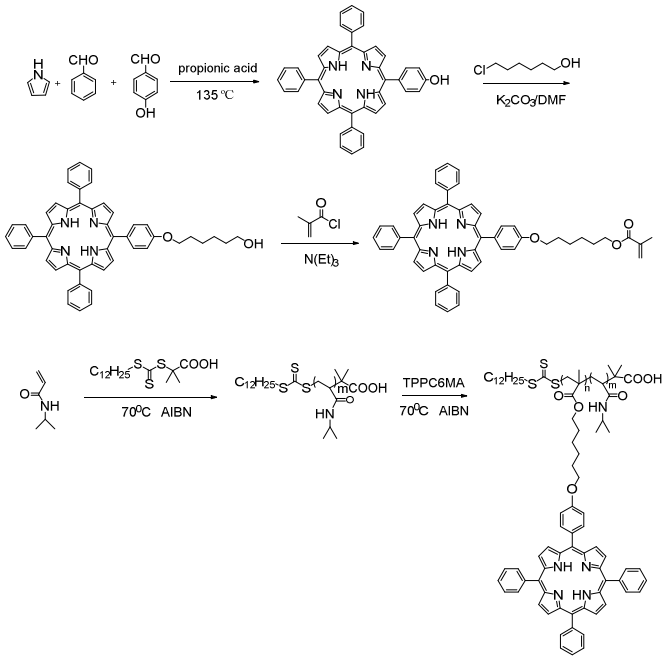

Scheme 1. Synthesis of PNIPAM-*b*-PTPPC6MA block copolymer.

Experimental

Materials

N-Isopropylacrylamide (NIPAM, Aldrich) was purified by recrystallization from a mixture of benzene and n-hexane. 4, 4′-Azobis(isobutyronitrile) (AIBN) (Fluka, 98%) were purified by recrystallization from ethanol. Tetrahydrofuran (THF) was dried by refluxing with the fresh sodium-benzophenone complex under N_2 and distilled just before use. 4′, 6-Diamidino-2-phenylindole (DAPI) and 3-(4, 5-dimethylthiazol-2-yl)-2, 5-diphenyltetrazolium bromide (MTT) were purchased from Aladdin and used as received. *S*-1-dodecyl-*S*′-(α,α′-dimethyl-α″-acetic acid) trithiocarbonate (DDAT) was prepared according to the previous literature.[36] All other reagents and solvents were of analytical grade and used as received unless mentioned.

Synthesis of 5-(4-Hydroxylphenyl)-10, 15, 20-triphenylporphyrin (TPP-OH)

5-(4-Hydroxylphenyl)-10, 15, 20-triphenylporphyrin was synthesized according to the previous literature.[37] Benzaldehyde (5.47 mL, 54 mmol) and p-hydroxybenzaldehyde (2.20 g, 18 mmol) were dissolved in propionic acid (240 mL). This solution was placed in a three-necked flask with a reflux condenser and magnetic stirring bar, and then was heated to 135 °C for 4 h. Then freshly distilled pyrrole (5 mL, 72 mmol) was added drop-wise to the solution under argon. The reaction mixture was heated to reflux for another 4 h and then cooled to room temperature. Then about half volume of reaction mixture was removed and methanol (200 mL) was added to the concentrated solution. This solution was stored overnight in a refrigerator, and then the purple precipitation was filtered off and washed with cold methanol. The crude product was purified on a silica gel column with chloroform/methanol (95:5, v/v) as the eluent. Yield: 0.53 g (4.59 %). ^{1}H NMR (400 MHz, $CDCl_3$), δ ppm: 8.86 (m, 8H, *β*-H), 8.21 (m, 6H, 10, 15, 20-Ar-*o*-H), 8.08 (m, 2H, 5-Ar-*o*-H), 7.75 (m, 9H, 10, 15, 20-Ar-*m*- and *p*-H), 7.22 (m, 2H, 5-Ar-*m*-H), -2.77 (s, 2H, -N*H*-).

Synthesis of 6-(5′-(4′-Phenoxyl)-10′, 15′, 20′-triphenylporphyrin)-1-hexanol (TPPC6-OH)

TPPC6-OH was synthesized from 5-(4-hydroxylphenyl)-10, 15, 20-triphenylporphyrin and 6-chloro-1-hexanol.[38] Briefly, TPP-OH (0.63 g, 1 mmol), 6-chloro-1-hexanol (0.15 mL, 1.15 mmol) and potassium carbonate (0.14 g, 1 mmol) were dissolved in 100 mL DMF. The mixture solution was refluxed for 12 h and washed with water three times. The product was extracted with dichloromethane, and dried with anhydrous $MgSO_4$. After the solvent was removed by evaporation, the crude product was purified on a silica gel column with dichloromethane as the eluent. Yield: 0.67 g (91.8 %). ^{1}H NMR (400 MHz, $CDCl_3$), δ ppm: 8.87 (m, 8H, *β*-H), 8.21 (m, 6H, 10, 15, 20-Ar-*o*-H), 8.11 (m, 2H, 5-Ar-*o*-H), 7.76 (m, 9H, 10, 15, 20-Ar-*m*- and *p*-H), 7.28 (m, 2H, 5-Ar-*m*-H), 4.26 (t, 2H, -O-CH_2-CH$_2$-), 3.75 (t, 2H, -CH_2-OH), 2.00 (m, 2H, -O-CH$_2$-CH_2-CH$_2$-), 1.76-1.59 (m, 6H, -CH$_2$-(CH_2)$_3$-CH$_2$-OH), -2.77 (s, 2H, -N*H*-).

Synthesis of 6-(5′-(4′-Phenoxyl)-10′, 15′, 20′-triphenylporphyrin) Methacrylate (TPPC6MA)

TPPC6MA was prepared by acylation of TPPC6-OH with methacryloyl chloride.[39] Typically, TPPC6-OH (0.365 g, 0.5 mmol), triethylamine (0.06 g, 0.6 mmol), and anhydrous THF (20 mL) were charged into a 50 mL flask. The mixture solution was cooled to 0 °C in an ice-water bath, and then methacryloyl chloride (0.062 g, 0.6 mmol) in 5 mL anhydrous THF was added dropwise into the solution under magnetic stirring. The mixture solution was stirred overnight at room temperature. After filtrating and evaporating the solvent, the residue was diluted with dichloromethane (DCM), washed with brine three times, and then dried with anhydrous $MgSO_4$. The crude product was finally purified by silica gel column with chromatograph using dichloromethane as the eluent. Yield: 0.37 g (92.5 %). ^{1}H NMR (400 MHz, $CDCl_3$): δ ppm: 8.87 (m, 8H, *β*-H), 8.21 (m, 6H, 10, 15, 20-Ar-*o*-H), 8.11 (m, 2H, 5-Ar-*o*-H), 7.76 (m, 9H, 10, 15, 20-Ar-*m*- and *p*-H), 7.28 (m, 2H, 5-Ar-*m*-H), 6.15 (s, 1H, HC*H*=C(CH_3)-), 5.59 (s, 1H, *H*CH=C(CH_3)-), 4.26 (m, 4H, -O-CH_2-CH_2-, -CH_2-CH_2-O-), 2.01 (m, 2H, -O-CH2-C*H*2-CH2-), 1.99 (s, 3H, -C*H*3), 1.84-1.61 (m, 6H, -CH_2-(CH_2)$_3$-CH_2-OH), -2.77 (s, 2H, -N*H*-).

Synthesis of PNIPAM Homopolymer

Poly(*N*-isopropylacrylamide) (PNIPAM) homopolymer was synthesized by RAFT polymerization using DDAT as the RAFT agent. NIPAM (1.0 g, 8.84 mmol), DDAT (0.022 g, 0.0603 mmol), AIBN (1.0 mg, 0.0061 mmol) and THF (2 mL) were charged into a 10 mL flask. The solution in the glass flask was degassed by three freeze-evacuate-thaw cycles, and then the glass tube was sealed under vacuum. The polymerization was carried out in an oil bath at 65 °C for 24 h and then quenched by liquid nitrogen. The reaction solution was precipitated in cold diethyl ether 3 times, and dried under vacuum. After dialysis, the product was concentrated and dried under vacuum. Finally, the white solid product of PNIPAM was obtained. Yield: 0.98 g (95.9%). M_n = 9 100 g/mol, M_w/M_n = 1.12.

Synthesis of PNIPAM-*b*-PTPPC6MA Block Copolymer

PNIPAM can be used as the macro-RAFT agent for the subsequent RAFT polymerization of TPPC6MA to produce the PNIPAM-*b*-PTPPC6MA block copolymers. A representative example of the synthesis of the PNIPAM-*b*-PTPPC6MA block copolymer is as follows: TPPC6MA (0.16 g, 0.2 mmol), PNIPAM (0.029 g, 0.002 mmol), AIBN (0.02 mg, 0.0012 mmol) and THF (1 mL) were placed in a dry glass tube equipped with a magnetic stirring bar. The mixture was degassed by at least three freeze-pump-thaw cycles. After the tube was flame-sealed under vacuum, it was stirred in an oil bath at 65 °C for 24 h and stopped by plunging the tube into liquid nitrogen. The solution was precipitated in cold diethyl ether and dried under vacuum, and then the purple solid product was obtained. Yield: 0.054 (29.4%). M_n = 24 500 g/mol, M_w/M_n = 1.18.

Preparation of Micelles in Aqueous Solution

In a typical procedure, the block copolymer (10 mg) was dissolved in 5.0 mL of THF. The solution was added dropwise into deionized water (20 mL) under magnetic stirring and then dialyzed against 2 L of water for 24 h using dialysis membrane (MWCO = 12 000) to remove the organic solvents. Then, the micelles solution was frozen and lyophilized to obtain freeze-dried powder by a freeze dryer system.

Critical Micelle Concentration (CMC) of Micelles

To estimate the CMC of the micelles, pyrene was used as the fluorescence probe.[40] A predetermined amount of pyrene in acetone was added into a series of volumetric flasks, and the acetone was allowed to evaporate. A predetermined volume of copolymer solutions and ultrapure water were added into the volumetric flasks to get solutions of different concentrations, while the concentration of pyrene in each flask was fixed at 6.0 × 10^{-7} mol/L. Fluorescence spectra were recorded using F-4500 fluorescence spectrometer and an excitation wavelength at 335 nm. Fluorescence emissions at 372 nm and 383 nm were monitored. The CMC was estimated as the cross-point when extrapolating the intensity ratio I_{372}/I_{383} at low and high concentration regions.

Singlet Oxygen Quantum Yields

Singlet oxygen quantum yield (Φ_Δ) was carried out according to the previous literature.[41-43] The Φ_Δ values were determined using 1, 3-diphenylisobenzofuran (DPBF) as a scavenger. The quantum yield of $^1O_2$ generation by PNIPAM-*b*-PTPPC6MA block copolymer was determined by comparing with TPP as a standard, which has a quantum yield of 0.62 in CCl_4.[44] The DPBF decay at 410 nm was monitored every 5 s. The singlet oxygen quantum was calculated according to Eq. (1):

$$\Phi_\Delta = \Phi_\Delta^{Std} \frac{R I_{abs}^{Std}}{R^{Std} I_{abs}} \quad (1)$$

Where, Φ_Δ^{Std} is the singlet oxygen quantum yields for the standard TPP (Φ_Δ^{Std} = 0.62 in CCl_4); R and R^{Std} are the DPBF photobleaching rates in the presence of the analyte and the standard, respectively; I_{abs} and I_{abs}^{Std} are the rates of light absorption by the analyte and the standard, respectively. To avoid chain reactions induced by quenchers (DPBF) in the presence of singlet oxygen, the concentration of the quencher (DPBF) was lowered than 3 × 10^{-5} M. The experiments were carried out in CCl_4.

Cell Culture

MCF-7 human breast adenocarcinoma line were cultivated in Dulbecco's modified Eagle's medium (DMEM) containing 10% fetal bovine serum (FBS) and antibiotics (50 units/mL penicillin and 50 units/mL streptomycin) at 37 °C under a humidified atmosphere containing 5% CO_2.

Cellular Uptake Studies

The cellular uptake behavior of PNIPAM-*b*-PTPPC6MA micelles and free porphyrin were monitored with flow cytometry and confocal laser scanning microscopy (CLSM), respectively. For flow cytometry analysis, MCF-7 cells were seeded in six-well flat culture plates with cell density of 1 × 10^6 cells/well. After 24 h incubation, the cells were treated with free porphyrin and PNIPAM-*b*-PTPPC6MA micelles for either 4 h or 24 h at the final concentration of porphyrin of 50 μg/mL. Then, the cells were trypsinized and prepared in suspension for flow cytometry analysis. The cells were resuspended in PBS and measured for the fluorescence intensity on a BD FACS Calibur flow cytometer, and the data analyzed with FlowJo software.

For CLSM measurement, MCF-7 cells were seeded on sterile cover glasses inserted in six-well plates at 5 × 10^4 cells/well in

1 mL of complete DMEM for 24 h. Prescribed amounts of PNIPAM-*b*-PTPPC6MA micelles were added and cells were incubated for 4 h and 24 h, respectively. After the culture medium was removed, the cells were washed with PBS three times. Thereafter, the cells were fixed with 4% paraformaldehyde for 30 min and washed with PBS three times. Finally, the cells were stained with 4′, 6-diamidino-2-phenylindole (DAPI) for 3 min and washed with PBS three times. After washing, the cover glasses were placed onto slides for imaging with confocal laser scanning microscope (Nikon AIR).

Dark Cytotoxicity of PNIPAM-*b*-PTPPC6MA Micelles

MCF-7 cells were chosen to evaluate the dark cytotoxicity of PNIPAM-*b*-PTPPC6MA micelles. The cells were seeded in a 96-well plate at a density of 4×10^3 cells/well. After culturing for 24 h, the MCF-7 cells were respectively treated with PNIPAM-*b*-PTPPC6MA micelles and free porphyrin at different dose in DMEM at 37 °C for 24 h in the dark, washed with sterilized PBS for three times, and the PNIPAM-*b*-PTPPC6MA or free porphyrin solution was replaced with fresh DMEM and 20 μL of 3-(4, 5-dimethylthiazol-2-yl)-2, 5-diphenyltetrazolium bromide (MTT) solution (5 mg/mL) for 4 h. Afterward, the MTT-containing medium was aspirated, and 150 μL of DMSO was added to each well to extract the formazan products with gentle agitation for 10 min. The absorbance at 492 nm was detected with a spectrophotometric microplate reader (THERMO Multiskan MK3 spectrometer). The cell viability was calculated as follows: cell viability (%) = $(OD_{test})/(OD_{control}) \times 100$, where OD_{test} was the absorbance at the presence of sample solutions, and $OD_{control}$ was the absorbance without treatment.

In Vitro Phototoxicity of PNIPAM-*b*-PTPPC6MA Micelles

The vitro phototoxicity of PNIPAM-*b*-PTPPC6MA was evaluated using above similar procedure for the dark cytotoxicity. After the addition of photosensitizing micelles into plates, all procedures were carried out in subdued light. The plate with cells was exposed to light from a visible light emitting diodes (LEDs) lamp (400 mW/cm^2) for 20 min. Irradiated cells were then incubated at 37 °C for 24 h, and cell viability was also evaluated using MTT assay.

Characterization

^{1}H NMR analysis was recorded on a BRUKER AV400 Spectrophotometer with $CDCl_3$ as solvent. Tetramethylsilane (TMS) was used as the internal reference. TEM studies were performed with a JEOL JEM 1400 instrument at a voltage of 100 KV. Samples were prepared by drop-casting micellar solutions onto carbon-coated copper grids and then air-drying at room temperature before measurement. The number-average molecular weight (M_n) and the polydispersity (M_w/M_n) were determined by GPC, which was measured on Waters 1515. The GPC system was calibrated using polystyrene as the standards and tetrahydrofuran (THF) was used as the eluent at a flow rate of 1 mL/min. DLS measurements were performed with a BECKMAN COULTER Delasa Nano C particle analyzer. All samples (0.2 mg/mL) were measured in aqueous solution at room temperature (25 °C) and at a scattering angle of 165°.

Results and Discussion

Synthesis of PNIPAM-*b*-PTPPC6MA Block Copolymers

To prepare the porphyrin monomer (**Scheme 1**), the mono-functional porphyrin compound, TPP-OH was synthesized first (**Fig. S1**). Considering the steric hindrance of porphyrin monomer in free-radical polymerization, the hydroxyl group of TPP-OH was extended to produce TPPC6-OH using 6-chloro-1-hexanol (**Fig. S2**), and the porphyrin monomer, TPPC6MA was finally synthesized by the acylation reaction between TPPC6-OH and methacryloyl chloride. The ^{1}H NMR spectrum of TPPC6MA was shown in **Fig. S3**. Besides the signals at 8.87-7.28 ppm and -2.77 ppm assigned to aromatic and pyrrole ring protons, and the signals at 4.26 ppm (i), 2.01 ppm (j), 1.84-1.61 ppm (l) assigned to the methylene protons, the signals at 6.15 ppm (g), 5.59 ppm (h), 1.99 ppm (k) are ascribed to the protons of methacrylate group (HCH=C(CH3)-).

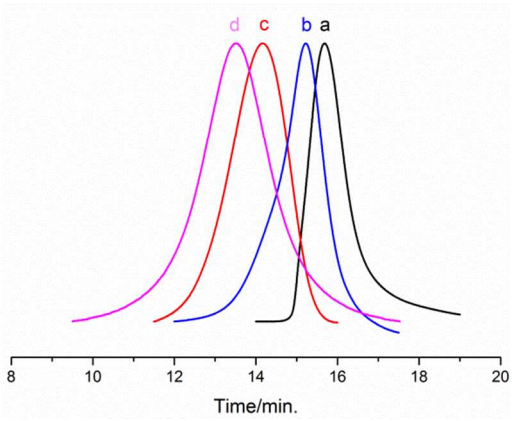

Fig. 1. GPC traces of (a) $PNIPAM_{130}$-DDAT, (b) $PNIPAM_{130}$-*b*-$PTPPC6MA_5$, (c) $PNIPAM_{130}$-*b*-$PTPPC6MA_{18}$ and (d) $PNIPAM_{130}$-*b*-$PTPPC6MA_{37}$.

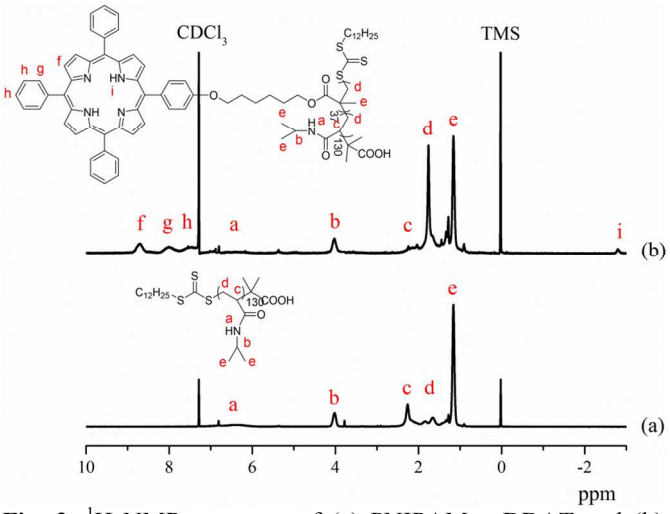

Fig. 2. ^{1}H NMR spectrum of (a) $PNIPAM_{130}$-DDAT and (b) $PNIPAM_{130}$-*b*-$PTPPC6MA_{37}$ in $CDCl_3$.

More recently, RAFT polymerization has been widely used to construct well-defined polymers, since it can be applied to the polymerization of a broad range of monomers containing polar groups such as carboxyl, amino and ionic groups.[45] For the monomer TPPC6MA, it contains pyrrole ring, so it is not suitable for other living polymerization approaches such as

atom transfer radical polymerization (ATRP). Thus, TPPC6MA was utilized to prepare the amphiphilic porphyrin-containing block copolymers via RAFT polymerization. The block copolymer was prepared in two steps. The hydrophiphilic block PNIPAM was first synthesized using DDAT as a chain transfer agent (CTA), and PNIPAM was further applied as the macro-RAFT agent for the subsequent RAFT polymerization of TPPC6MA to produce PNIPAM-*b*-PTPPC6MA block copolymers (**Scheme 1**). The PNIPAM-*b*-PTPPC6MA block copolymers with different block lengths of PTPPC6MA were synthesized by varying the ratio of TPPC6MA to PNIPAM-DDAT RAFT agent. The results of the polymerization of block copolymers were summarized in **Table 1**. The GPC was first used to characterize the polymerization of these block copolymers. As can be seen from the GPC curves shown in **Fig. 1**, the eluograms of PNIPAM-*b*-PTPPC6MA shift to lower elution volume with increasing the length of PTPPC6MA chain, compared to that of macro-RAFT agent (PNIPAM), moreover, the peaks of the PNIPAM-*b*-PTPPC6MA block copolymers are symmetrical, and their PDI are also quite lower (less than 1.23), which suggests the RAFT polymerization of TPPC6MA is living/well-controlled. The ^{1}H NMR spectrum of PNIPAM$_{130}$-*b*-PTPPC6MA$_{37}$ block copolymer was shown in **Fig. 2**, The signals at 5.8-7.0 ppm (a) and 4.02 ppm (b) are respectively assigned to the protons of -N*H*- and $(CH_3)_2$-C*H*-NH- from block PNIPAM, and the signals at 8.72 ppm (f), 8.01 ppm (g), 7.72-7.36 ppm (h) and -2.79 ppm (i) are ascribed to the protons from block PTPPC6MA. Based on the ^{1}H NMR and GPC results, the well-defined amphiphilic PNIPAM-*b*-PTPPC6MA block copolymers was successfully achieved via RAFT polymerization.

Table 1. The results of the polymerization of block copolymers

Polymer	$M_{n,th}$[c] (g mol^{-1})	$M_{n,GPC}$[d] (g mol^{-1})	PDI[d]
PNIPAM$_{130}$-DDAT	14 700	9 000	1.12
PNIPAM$_{130}$-*b*-PTPPC6MA$_5$	18 700	15 100	1.12
PNIPAM$_{130}$-*b*-PTPPC6MA$_{18}$	29 100	24 500	1.18
PNIPAM$_{130}$-*b*-PTPPC6MA$_{37}$	44 300	38 600	1.23

[a]PNIPAM$_{130}$-DDAT prepared using DDAT as the RAFT agent.
[b]PNIPAM-*b*-PTPPC6MA prepared using PNIPAM$_{130}$-DDAT as RAFT agent.
[c]$M_{n,th} = M_{w,\ monomer} \times ([monomer]_0/[macro\text{-}CTA]_0) \times x + M_{w,\ macro\text{-}CTA}$, where $M_{w,\ monomer}$, and $M_{w,\ macro\text{-}CTA}$ are the molecular weights of TPPC6MA and PNIPAM$_{130}$-DDAT, respectively; x is the weight conversion.
[d]Number-average weight ($M_{n,GPC}$) and molecular weight distribution (PDI = M_w/M_n) evaluated by GPC.

Micelles Formation and Characterization

The self-assembly behaviors of amphiphilic block copolymers in selective solution have attracted considerable interest in recent years, since a rich variety of self-assembled morphologies could be achieved such as micelles and vesicles, and they exhibited the potential applications in drug delivery systems, sensor systems, and functional nanomaterials.[33,46-49] Here, the self-assembly of porphyrin-containing amphiphilic PNIPAM-*b*-PTPPC6MA block copolymer was studied in aqueous solution. Samples were prepared by adding PNIPAM-*b*-PTPPC6MA block copolymer THF solution into deionized water under magnetic stirring, and then dialyzed against deionized water to remove THF. The critical micelle concentrations (CMC) of these block copolymers in water were measured by fluorescence spectra using pyrene as a hydrophobic probe, since pyrene can transfer from the aqueous environment to hydrophobic region of the micelle interior core, resulting in significant spectroscopic changes. As shown in **Fig. 3**, the I_{383}/I_{372} ratio remained almost unchanged at low copolymer concentrations but increased sharply when the copolymer concentrations reached a certain value, indicating the pyrene was trapped into the micelle core with more hydrophobic environment, which is actually a reflection of micelle formation. The CMC values of these copolymers were listed in **Table 2**. We can clearly see that the CMC decreased with the increase of the length of PTPPC6MA. This is because the increase of the length of hydrophobic block PTPPC6MA promotes the formation of polymeric micelles.

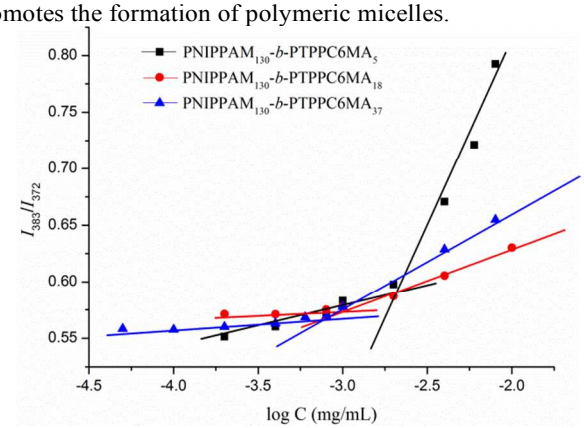

Fig. 3. Plot of the I_{383}/I_{372} ratio against log C of amphiphilic polymers in deionized water.

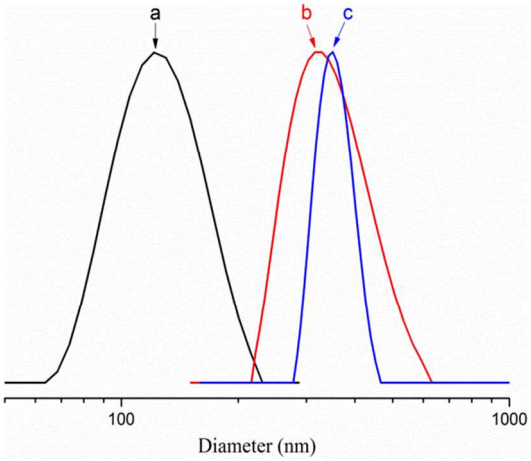

Fig. 4. Size distributions of (a) PNIPAM$_{130}$-*b*-PTPPC6MA$_5$, (b) PNIPAM$_{130}$-*b*-PTPPC6MA$_{18}$ and (c) PNIPAM$_{130}$-*b*-PTPPC6MA$_{37}$ micelles in aqueous solution.

Table 2. Characterization of Polymeric Micelles

Samples	D_h (nm)[a]	PDI[a]	CMC (mg/mL)[b]	LCST (^{o}C)[a]
PNIPAM$_{130}$-*b*-PTPPC6MA$_5$	119.2	0.072	2.04	31.2
PNIPAM$_{130}$-*b*-PTPPC6MA$_{18}$	324.3	0.093	0.96	29.7
PNIPAM$_{130}$-*b*-PTPPC6MA$_{37}$	347.5	0.014	0.79	27.3

[a]Determined by DLS.
[b]CMC was determined by a fluorescence spectroscopic method using pyrene as the fluorescence probe.

The self-assembled morphologies of PNIPAM-*b*-PTPPC6MA block copolymers in water were then characterized by TEM. **Fig. 5a** showed spherical micelles formed from PNIPAM$_{130}$-*b*-PTPPC6MA$_5$. This is typical core-

shell assembled micelles with hydrophobic block PTPPC6MA as the core and hydrophilic block PNIPAM as the corona. Additionally, the assembled micelles were also studied by dynamic light scattering (DLS) as shown in **Fig. 4**. The apparent hydrodynamic diameters (D_h) of PNIPAM$_{130}$-*b*-PTPPC6MA$_5$ micelles is 119.2 nm which is considerably larger than that measured by TEM. This can be attributed to the fact that the PNIPAM chains are extended in solution. Upon increasing the hydrophobic PTPPC6MA block length for PNIPAM$_{130}$-*b*-PTPPC6MA$_{18}$, large vesicular aggregates with the size of 324.3 nm were obtained in **Fig. 5b**. Interestingly, with further increasing the length the TPPC6MA, PNIPAM$_{130}$-*b*-PTPPC6MA$_{37}$, could form a single large vesicle with the diameter around 347.5 nm, and the wall thickness about 25 nm (**Fig. 5c**). The DLS was also employed to evaluate the stability of PNIPAM-*b*-PTPPC6MA micelles in PBS at 37 °C. As shown in Fig. S7 and Table S3, these PNIPAM-*b*-PTPPC6MA micelles are well stabile in PBS at 37 °C.

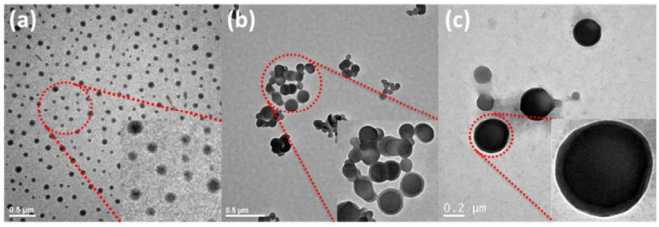

Fig. 5. TEM images of (a) PNIPAM$_{130}$-*b*-PTPPC6MA$_5$ (scale bar, 500 nm), (b) PNIPAM$_{130}$-*b*-PTPPC6MA$_{18}$ (scale bar, 500 nm) and (c) PNIPAM$_{130}$-*b*-PTPPC6MA$_{37}$ (scale bar, 200 nm).

The self-assembled morphology of amphiphilic polymers is mainly dependent on polymer composition, namely the block length ratio between hydrophobic block and hydrophilic block.[50-52] In our case, the self-assembled morphologies of PNIPAM-*b*-PTPPC6MA were greatly influenced by the mass ratios of hydrophobic PTPPC6MA block to hydrophilic PNIPAM block, which is similar to the previous result reported by Eisenberg *et al*.[53] The stretching degree plays an important role for the size of micelles via entropy penalty, and the hydrophobic PTPPC6MA chains were random stretching inside the core of micelles. With the mass ratio of PTPPC6MA to PNIPAM increasing from 0.3:1 to 1:1, the morphologies clearly changed from spheres to vesicular aggregates. PTPPC6MA chains in the PNIPAM$_{130}$-*b*-PTPPC6MA$_{18}$ vesicles were more incompact than those in PNIPAM$_{130}$-*b*-PTPPC6MA$_5$ spherical micelles as a result of hydrophobic chains stretching degree increasing. Additionally, the hydrophobic PTPPC6MA block could also increase the space between coronal domains and decrease the interaction between inter coronal chains, forming the vesicular aggregates. Upon further increasing the mass ratio of PTPPC6MA to PNIPAM to 2:1, vesicles aggregates could change to single vesicles under similar assembled conditions due to further decrease of the stretching degree and increase of corona repulsion.[54-57] Consequently, the self-assembled morphologies of PNIPAM-*b*-PTPPC6MA in aqueous solution could vary from spheres to vesicular aggregates and then to single vesicles with the chain length of PTPPC6MA block increasing (**Scheme 2a**).

PNIPAM is a known thermosensitive polymer, and the linear free homo-PNIPAM in aqueous solution has a sharp phase transition with the lower critical solution temperature (LCST) at about 32 °C. Here, the phase transition behavior of all the block copolymers was studied by DLS. **Fig. 6** shows temperature-dependent D_h of the three different copolymers. Each data point was obtained after the measured values were stable. It can be clearly seen that D_h of block polymer micelles gradually decreases with the temperature, exhibiting a broad transition for the three samples. The similar phenomenon was also found in our previous work of PNIPAM-*b*-PS block copolymers.[58] Additionally, we also could find that the LCST decreases from 31.2 °C to 29.7 °C and then 27.3 °C with increasing block length the PTPPC6MA.

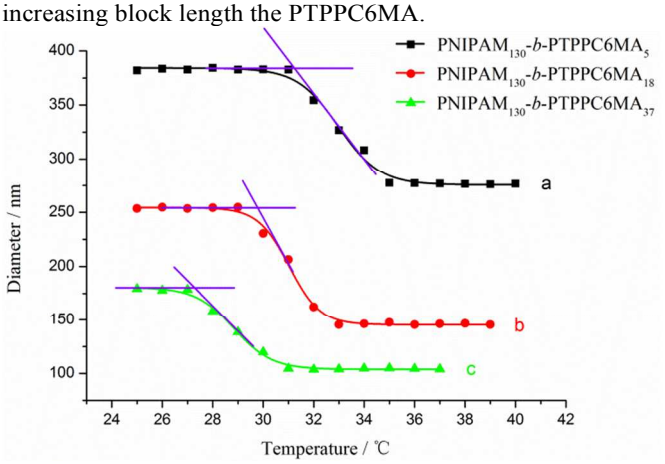

Fig. 6. Temperature dependence of the hydrodynamic diameter D_h of: (a) PNIPAM$_{130}$-*b*-PTPPC6MA$_5$, (b) PNIPAM$_{130}$-*b*-PTPPC6MA$_{18}$ and (c) PNIPAM$_{130}$-*b*-PTPPC6MA$_{37}$ in aqueous solution.

Table 3. Singlet oxygen quantum yield of PNIPAM-*b*-PTPPC6MA block copolymers in CCl_4.

Samples	Φ_Δ
PNIPAM$_{130}$-*b*-PTPPC6MA$_5$	0.769
PNIPAM$_{130}$-*b*-PTPPC6MA$_{18}$	0.787
PNIPAM$_{130}$-*b*-PTPPC6MA$_{37}$	0.812
TPP	0.62

Singlet Oxygen Quantum Yields

It is well known that the singlet oxygen could be produced when the energy transfer between the triplet state and ground state of photosensitizers. Thus it is aspired that a high efficiency of energy transfer between excited triplet state of porphyrin and the ground state of oxygen to generate large amounts of singlet oxygen.[2] The singlet oxygen quantum yield (Φ_Δ) values were determined using a chemical method that the DPBF as a quencher and TPP as a standard. The peak intensity of the mixture of quenchers (DPBF) and PNIPAM$_{130}$-*b*-PTPPC6MA$_{37}$ in CCl_4 was monitored using UV–Vis spectrophotometer (**Fig. 7**). The singlet oxygen quantum of PNIPAM$_{130}$-*b*-PTPPC6MA$_{37}$ was calculated according to Eq. (1), and the result was listed in **Table 3**. It can be seen that the singlet oxygen quantum yields of block copolymers are slightly higher than that of the standard TPP, indicating that the block copolymers bearing porphyrin moieties are better for the singlet oxygen formation.

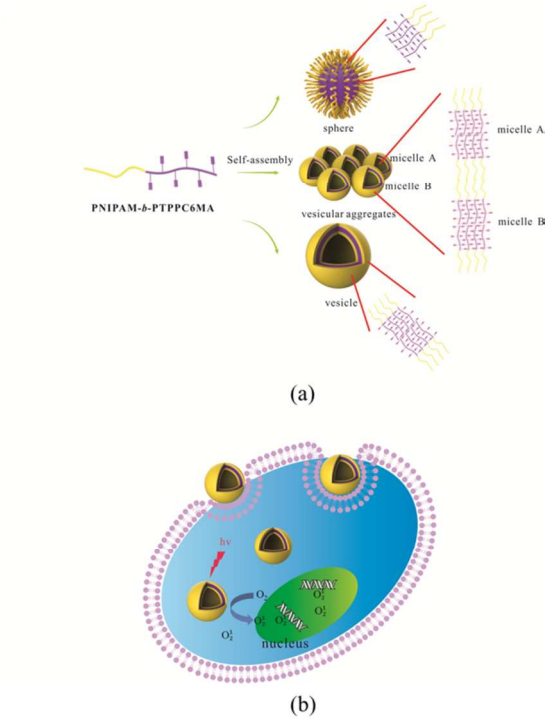

Scheme 2. (a) Self-assembly of PNIPAM-*b*-PTPPC6MA amphiphiles into three kinds of morphologies: sphere, vesicular aggregates and large vesicle. (b) Vesicle of $PNIPAM_{130}$-*b*-$PTPPC6MA_{37}$ amphiphiles for intracellular photodynamic therapy.

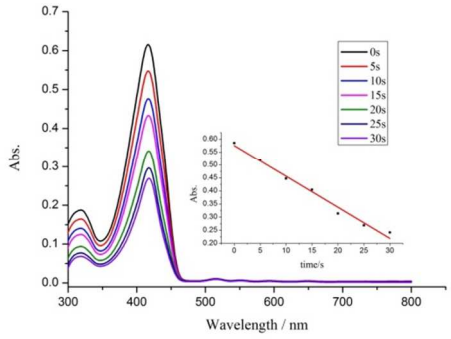

Fig. 7. UV-Vis absorption spectra of DPBF with $PNIPAM_{130}$-*b*-$PTPPC6MA_{37}$ after irradiation for different times (inset: plot of absorbance versus concentration).

Cellular Uptake of PNIPAM-*b*-PTPPC6MA Micelles

The cellular internalization of free TPP and PNIPAM-*b*-PTPPC6MA micelles in MCF-7 cells at 4 h and 24 h of post-treatment was evaluated by flow cytometry and confocal laser scanning microscopy (CLSM), respectively. As shown in **Fig. 8**, the fluorescence of porphyrin in cells at different time (4 h and 24 h) was quantitatively analyzed with flow cytometry. After 4 h incubation with free TPP and $PNIPAM_{130}$-*b*-$PTPPC6MA_{37}$ micelles, the fluorescence intensity of $PNIPAM_{130}$-*b*-$PTPPC6MA_{37}$ was apparently stronger than that of free TPP. The similar result also can be found in incubating for 24 h. Moreover, the fluorescence intensity at 24 h was much higher than that at 4 h for each sample (**Fig. S9**). Additionally, the fluorescence intensities of these micelles incubated cells were all stronger than that of free porphyrin. The time-dependent and enhanced cellular uptake of porphyrin by PNIPAM-*b*-PTPPC6MA micelles could be attributed to the fact that free TPP can be transported into cells via diffusion, while the PNIPAM-*b*-PTPPC6MA micelles may be taken up by cells via the endocytosis process.[59,60]

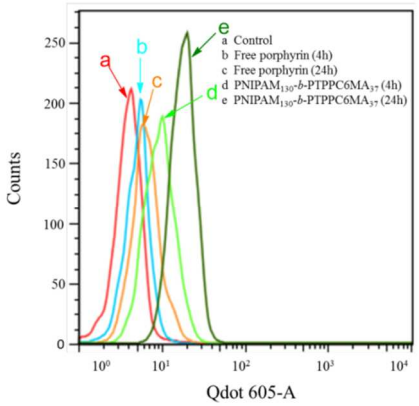

Fig. 8. Flow cytometric demonstration of MCF-7 cells after incubation with (a) control, (b) free porphyrin for 4 h, (c) free TPP for 24 h, (d) $PNIPAM_{130}$-*b*-$PTPPC6MA_{37}$ for 4 h, and (e) $PNIPAM_{130}$-*b*-$PTPPC6MA_{37}$ for 24 h.

The cellular uptake behaviors of PNIPAM-*b*-PTPPC6MA micelles by MCF-7 cells were further investigated by CLSM (**Fig. 9**). MCF-7 cells treated with $PNIPAM_{130}$-*b*-$PTPPC6MA_{37}$ micelles for 4 h showed slight red fluorescence in cytosol (**Fig. 9c**) while significantly higher fluorescence were obtained for 24 h (**Fig. 9d**). Comparing the intensity of red fluorescence between free porphyrin and $PNIPAM_{130}$-*b*-$PTPPC6MA_{37}$, we found that the fluorescence intensity of micelles treated with $PNIPAM_{130}$-*b*-$PTPPC6MA_{37}$ micelles were stronger than that treated with free porphyrin not only for 4 h but also 24 h. The same result also can be found for $PNIPAM_{130}$-*b*-$PTPPC6MA_5$ and $PNIPAM_{130}$-*b*-$PTPPC6MA_{18}$ micelles (**Fig. S10**). These results indicate that PNIPAM-*b*-PTPPC6MA micelles might be taken up by the cells through a nonspecific endocytosis mechanism.[61,62]

Vitro Dark Toxicity and Phototoxicity of PNIPAM-*b*-PTPPC6MA Micelles

To investigate the vitro phototoxicity of PNIPAM-*b*-PTPPC6MA micelles, the cytotoxicity against MCF-7 cells was determined by MTT assay after treatment with or without light (**Fig. 10**). Cells in the dark without PNIPAM-*b*-PTPPC6MA micelles treatment were set to the viability of 100% as a reference. Without light treatment, the three block copolymer micelles and free porphyrin displayed nearly no cytotoxicity in the range of 0.78~100 μg/mL (**Fig. 10a**). With light illumination, the phototoxicity occurred and became more intense with the increase in the feeding concentration of PNIPAM-*b*-PTPPC6MA micelles, indicating that the porphyrin-containing block copolymer micelles could effectively generate the cytotoxic substance to kill the cells, but the free porphyrin showed very low phototoxicity. Moreover, we found $PNIPAM_{130}$-*b*-$PTPPC6MA_{37}$ micelles with a long chain length of PTPPC6MA had a high effectiveness in PDT cell killing with IC50 of 22 μg/mL. This result was well agreement with the singlet oxygen quantum yields of these PNIPAM-*b*-PTPPC6MA micelles. Consequently, the

PNIPAM-*b*-PTPPC6MA amphiphilic copolymer may contribute to the development of a new generation of photosensitizer for PDT.

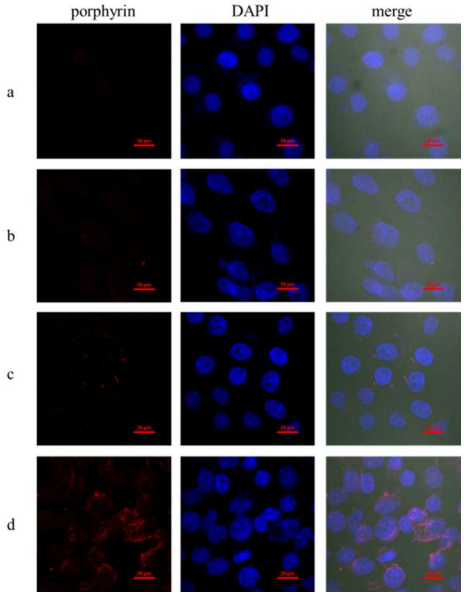

Fig. 9. CLSM images of MCF-7 cells incubated with free porphyrin for 4 h (a) and 24 h (b), and with PNIPAM$_{130}$-*b*-PTPPC6MA$_{37}$ micelles for 4 h (c) and 24 h (d), respectively. The images from left to right were the cells with porphyrin fluorescence, with nuclear staining with DAPI and overlays of images. Scale bar, 20 μm.

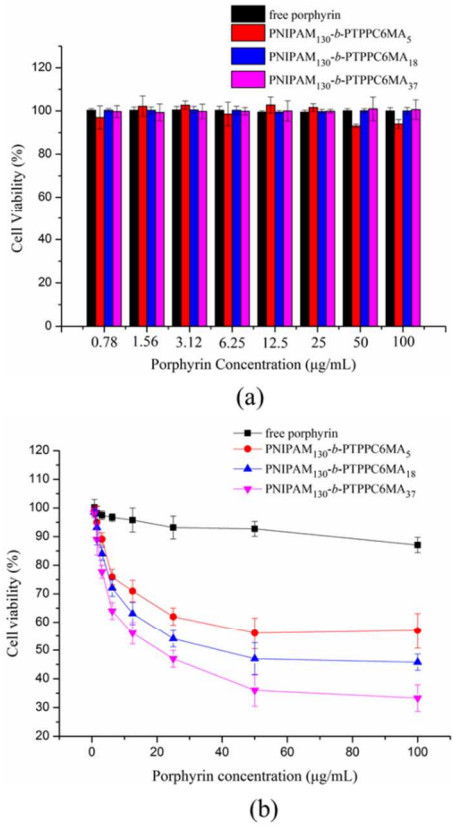

Fig. 10. Viability of MCF-7 cells determined by MTT assay after treatment of PNIPAM-*b*-PTPPC6MA micelles (a) dark toxicity and (b) phototoxicity.

Conclusions

A series of PNIPAM-*b*-PTPPC6MA block copolymers with different hydrophobic chain length of PTPPC6MA were successfully synthesized by using PNIPAM-DDAT as macro-RAFT agent. The morphologies of PNIPAM-*b*-PTPPC6MA micelles formed in water varied from sphere to vesicular aggregates to single large vesicle via increasing the length of hydrophobic chain. The results of CLSM and flow cytometry showed that PNIPAM-*b*-PTPPC6MA micelles were more efficiently internalized by MCF-7 cells than free porphyrin. According to the MTT assay, porphyrin-containing block copolymer micelles could effectively generate the cytotoxic substance to kill the cells, but the free porphyrin shows very low phototoxicity. Moreover, the phototoxicity of these micelles increases with the increasing content of hydrophobic chain PTPPC6MA which is well agreeable with the change trend of their singlet oxygen quantum yields. Therefore, PNIPAM-*b*-PTPPC6MA block copolymers would be a promising PS for PDT.

Acknowledgements

This work was financially supported by the National Natural Science Foundation of China (No. 51173044), Research Innovation Program of SMEC (No.14ZZ065), Shanghai Pujiang Program under 14PJ1402600, and the Open Funding Project of the State Key Laboratory of Bioreactor Engineering. W. Z. also acknowledges the support from the Fundamental Research Funds for the Central Universities.

Notes and references

State Key Laboratory of Bioreactor Engineering; Shanghai Key Laboratory of Advanced Polymeric Materials, East China University of Science and Technology, 130 Meilong Road, Shanghai 200237, China.

*Corresponding authors. Tel.:+86 21 64253033; Fax: +86 21 64253033.
Email: wazhang@ecust.edu.cn

(1) Celli, J. P.; Spring, B. Q.; Rizvi, I.; Evans, C. L.; Samkoe, K. S.; Verma, S.; Pogue, B. W.; Hasan, T. *Chemical Reviews* **2010**, *110*, 2795.

(2) Ethirajan, M.; Chen, Y. H.; Joshi, P.; Pandey, R. K. *Chemical Society Reviews* **2011**, *40*, 340.

(3) Lovell, J. F.; Liu, T. W. B.; Chen, J.; Zheng, G. *Chemical Reviews* **2010**, *110*, 2839.

(4) Nishiyama, N.; Morimoto, Y.; Jang, W. D.; Kataoka, K. *Advanced Drug Delivery Reviews* **2009**, *61*, 327.

(5) Rai, P.; Mallidi, S.; Zheng, X.; Rahmanzadeh, R.; Mir, Y.; Elrington, S.; Khurshid, A.; Hasan, T. *Advanced Drug Delivery Reviews* **2010**, *62*, 1094.

(6) Henderson, B. W.; Dougherty, T. J. *Photochemistry and Photobiology* **1992**, *55*, 145.

(7) Baek, S.; Na, K. *Colloids and Surfaces B-Biointerfaces* **2013**, *101*, 493.

(8) Usuda, J.; Kato, H.; Okunaka, T.; Furukawa, K.; Tsutsui, H.; Yamada, K.; Suga, Y.; Honda, H.; Nagatsuka, Y.; Ohira, T.; Tsuboi, M.; Hirano, T. *Journal of Thoracic Oncology* **2006**, *1*, 489.

(9) Wirotius, A.-L.; Ibarboure, E.; Scarpantonio, L.; Schappacher, M.; McClenaghan, N. D.; Deffieux, A. *Polymer Chemistry* **2013**, *4*, 1903.

(10) DeRosa, M. C.; Crutchley, R. J. *Coordination Chemistry Reviews* **2002**, *233–234*, 351.

(11) Liu, P.; Yue, C.; Sheng, Z.; Gao, G.; Li, M.; Yi, H.; Zheng, C.; Wang, B.; Cai, L. *Polymer Chemistry* **2014**, *5*, 874.

(12) Nakamura, H.; Liao, L.; Hitaka, Y.; Tsukigawa, K.; Subr, V.; Fang, J.; Ulbrich, K.; Maeda, H. *Journal of Controlled Release* **2013**, *165*, 191.

(13) Shan, J. N.; Budijono, S. J.; Hu, G. H.; Yao, N.; Kang, Y. B.; Ju, Y. G.; Prud'homme, R. K. *Advanced Functional Materials* **2011**, *21*, 2488.

(14) Oenbrink, G.; Jurgenlimke, P.; Gabel, D. *Photochemistry and Photobiology* **1988**, *48*, 451.

(15) Liu, Y.; Huang, Z.; Liu, K.; Kelgtermans, H.; Dehaen, W.; Wang, Z.; Zhang, X. *Polymer Chemistry* **2014**, *5*, 53.

(16) Huynh, E.; Lovell, J. F.; Helfield, B. L.; Jeon, M.; Kim, C.; Goertz, D. E.; Wilson, B. C.; Zheng, G. *Journal of the American Chemical Society* **2012**, *134*, 16464.

(17) Lovell, J. F.; Jin, C. S.; Huynh, E.; Jin, H. L.; Kim, C.; Rubinstein, J. L.; Chan, W. C. W.; Cao, W. G.; Wang, L. V.; Zheng, G. *Nature Materials* **2011**, *10*, 324.

(18) Ng, K. K.; Shakiba, M.; Huynh, E.; Weersink, R. A.; Roxin, Á.; Wilson, B. C.; Zheng, G. *ACS Nano* **2014**.

(19) Lovell, J. F.; Jin, C. S.; Huynh, E.; MacDonald, T. D.; Cao, W. G.; Zheng, G. *Angewandte Chemie-International Edition* **2012**, *51*, 2429.

(20) Li, F. Y.; Na, K. *Biomacromolecules* **2011**, *12*, 1724.

(21) Park, H.; Park, W.; Na, K. *Biomaterials* **2014**, *35*, 7963.

(22) Park, W.; Park, S. J.; Na, K. *Biomaterials* **2011**, *32*, 8261.

(23) Li, F.; Bae, B.-c.; Na, K. *Bioconjugate Chemistry* **2010**, *21*, 1312.

(24) de Loos, F.; Reynhout, I. C.; Cornelissen, J. J. L. M.; Rowan, A. E.; Nolte, R. J. M. *Chemical Communications* **2005**, 60.

(25) High, L. R. H.; Holder, S. J.; Penfold, H. V. *Macromolecules* **2007**, *40*, 7157.

(26) Shieh, M. J.; Hsu, C. Y.; Huang, L. Y.; Chen, H. Y.; Huang, F. H.; Lai, P. S. *Journal of Controlled Release* **2011**, *152*, 418.

(27) Li, Z. Y.; Wang, H. Y.; Li, C.; Zhang, X. L.; Wu, X. J.; Qin, S. Y.; Zhang, X. Z.; Zhuo, R. X. *Journal of Polymer Science Part a-Polymer Chemistry* **2011**, *49*, 286.

(28) Chen, W.; Zhong, P.; Meng, F. H.; Cheng, R.; Deng, C.; Feijen, J.; Zhong, Z. Y. *Journal of Controlled Release* **2013**, *169*, 171.

(29) Du, J.-Z.; Du, X.-J.; Mao, C.-Q.; Wang, J. *Journal of the American Chemical Society* **2011**, *133*, 17560.

(30) Hu, X.; Liu, S.; Huang, Y.; Chen, X.; Jing, X. *Biomacromolecules* **2010**, *11*, 2094.

(31) Hu, X. L.; Hu, J. M.; Tian, J.; Ge, Z. S.; Zhang, G. Y.; Luo, K. F.; Liu, S. Y. *Journal of the American Chemical Society* **2013**, *135*, 17617.

(32) Dai, J. A.; Zou, S. Y.; Pei, Y. Y.; Cheng, D.; Ai, H.; Shuai, X. T. *Biomaterials* **2011**, *32*, 1694.

(33) Kataoka, K.; Harada, A.; Nagasaki, Y. *Advanced Drug Delivery Reviews* **2001**, *47*, 113.

(34) Xu, J.; Liu, S. Y. *Soft Matter* **2008**, *4*, 1745.

(35) Li, Y. Y.; Zhang, X. Z.; Cheng, H.; Zhu, J. L.; Cheng, S. X.; Zhuo, R. X. *Macromolecular Rapid Communications* **2006**, *27*, 1913.

(36) Lai, J. T.; Filla, D.; Shea, R. *Macromolecules* **2002**, *35*, 6754.

(37) D'Souza, F.; Deviprasad, G. R.; El-Khouly, M. E.; Fujitsuka, M.; Ito, O. *Journal of the American Chemical Society* **2001**, *123*, 5277.

(38) Wang, S. H.; Shen, Q. X.; Nawaz, M. H.; Zhang, W. A. *Polymer Chemistry* **2013**, *4*, 2151.

(39) Dutta, P.; Dey, J.; Shome, A.; Das, P. K. *International Journal of Pharmaceutics* **2011**, *414*, 298.

(40) Kabanov, A. V.; Nazarova, I. R.; Astafieva, I. V.; Batrakova, E. V.; Alakhov, V. Y.; Yaroslavov, A. A.; Kabanov, V. A. *Macromolecules* **1995**, *28*, 2303.

(41) Brannon, J. H.; Magde, D. *Journal of the American Chemical Society* **1980**, *102*, 62.

(42) Ng, A. C. H.; Li, X. Y.; Ng, D. K. P. *Macromolecules* **1999**, *32*, 5292.

(43) SPILLER, W.; KLIESCH, H.; WÖHRLE, D.; HACKBARTH, S.; RÖDER, B.; SCHNURPFEIL, G. *Journal of Porphyrins and Phthalocyanines* **1998**, *02*, 145.

(44) Wilkinson, F.; Helman, W. P.; Ross, A. B. *Journal of Physical and Chemical Reference Data* **1993**, *22*, 113.

(45) Boyer, C.; Bulmus, V.; Davis, T. P.; Ladmiral, V.; Liu, J. Q.; Perrier, S. *Chemical Reviews* **2009**, *109*, 5402.

(46) Kakizawa, Y.; Kataoka, K. *Advanced Drug Delivery Reviews* **2002**, *54*, 203.

(47) Ma, P. X. *Advanced Drug Delivery Reviews* **2008**, *60*, 184.

(48) Schmaljohann, D. *Advanced Drug Delivery Reviews* **2006**, *58*, 1655.

(49) Zhang, W. A.; Muller, A. H. E. *Progress in Polymer Science* **2013**, *38*, 1121.

(50) Bhargava, P.; Zheng, J. X.; Li, P.; Quirk, R. P.; Harris, F. W.; Cheng, S. Z. D. *Macromolecules* **2006**, *39*, 4880.

(51) Mai, Y.; Eisenberg, A. *Chemical Society Reviews* **2012**, *41*, 5969.

(52) LaRue, I.; Adam, M.; Zhulina, E. B.; Rubinstein, M.; Pitsikalis, M.; Hadjichristidis, N.; Ivanov, D. A.; Gearba, R. I.; Anokhin, D. V.; Sheiko, S. S. *Macromolecules* **2008**, *41*, 6555.

(53) Zhang, L.; Eisenberg, A. *Journal of the American Chemical Society* **1996**, *118*, 3168.

(54) Chen, S.-C.; Kuo, S.-W.; Chang, F.-C. *Langmuir* **2011**, *27*, 10197.

(55) He, W.-D.; Sun, X.-L.; Wan, W.-M.; Pan, C.-Y. *Macromolecules* **2011**, *44*, 3358.

(56) Zehm, D.; Ratcliffe, L. P. D.; Armes, S. P. *Macromolecules* **2012**, *46*, 128.

(57) Zhang, L.; Eisenberg, A. *Science* **1995**, *268*, 1728.

(58) Zhang, W. A.; Zhou, X. C.; Li, H.; Fang, Y.; Zhang, G. Z. *Macromolecules* **2005**, *38*, 909.

(59) Yoo, H. S.; Lee, K. H.; Oh, J. E.; Park, T. G. *Journal of Controlled Release* **2000**, *68*, 419.

(60) Sahay, G.; Batrakova, E. V.; Kabanov, A. V. *Bioconjugate Chemistry* **2008**, *19*, 2023.

(61) Zhang, W.; Li, Y.; Liu, L.; Sun, Q.; Shuai, X.; Zhu, W.; Chen, Y. *Biomacromolecules* **2010**, *11*, 1331.

(62) Liu, J.; Huang, W.; Pang, Y.; Zhu, X.; Zhou, Y.; Yan, D. *Biomacromolecules* **2010**, *11*, 1564.